Short Article

Cell Host & Microbe

Helicobacter pylori Employs a Unique Basolateral Type IV Secretion Mechanism for CagA Delivery

Graphical Abstract

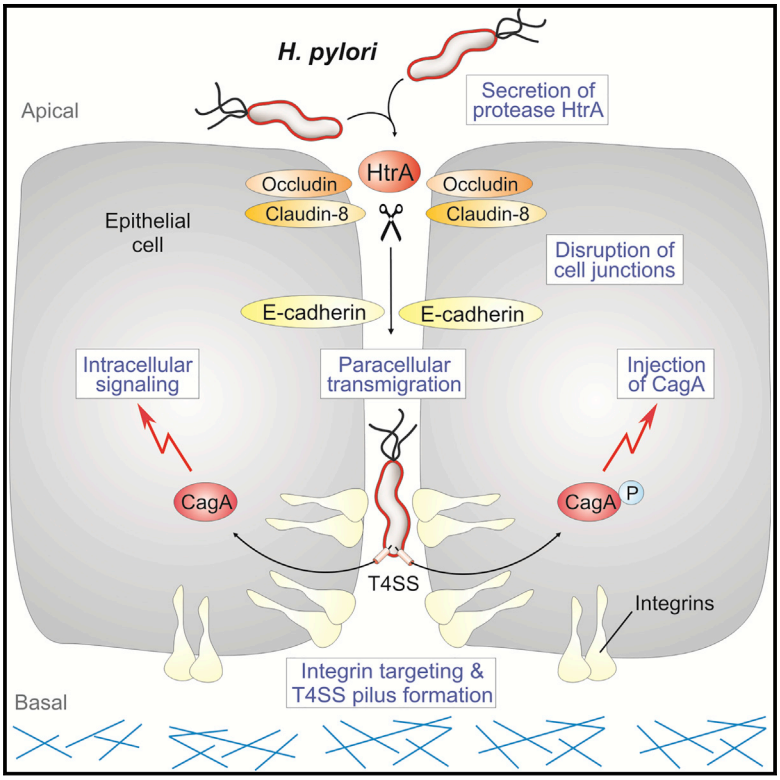

Highlights

- T4SS pilus formation during *H. pylori* (*Hp*) infection occurs at basolateral membranes
- *Hp* secretes HtrA, a serine protease that cleaves epithelial junctional proteins
- HtrA and opening of cell junctions are required for *Hp* paracellular transmigration
- The T4SS pilus is activated at basolateral membranes and injects CagA

Authors

Nicole Tegtmeyer, Silja Wessler, Vittorio Necchi, ..., Enrico Solcia, Vittorio Ricci, Steffen Backert

Correspondence

steffen.backert@fau.de

In Brief

The type IV secretion system of *Helicobacter pylori* requires basolateral integrin receptors for its function. Tegtmeyer et al. unravel that secreted serine protease HtrA opens cell-to-cell junctions by cleaving occludin, claudin-8, and E-cadherin. This allows bacterial transmigration across polarized epithelial cells to reach integrins for injecting CagA at basolateral membranes.

Tegtmeyer et al., 2017, Cell Host & Microbe *22*, 552–560
October 11, 2017
https://doi.org/10.1016/j.chom.2017.09.005

CellPress

Cell Host & Microbe
Short Article

Helicobacter pylori Employs a Unique Basolateral Type IV Secretion Mechanism for CagA Delivery

Nicole Tegtmeyer,[1] Silja Wessler,[2] Vittorio Necchi,[3] Manfred Rohde,[4] Aileen Harrer,[1] Tilman T. Rau,[5,6] Carmen Isabell Asche,[1] Manja Boehm,[1] Holger Loessner,[7] Ceu Figueiredo,[8] Michael Naumann,[9] Ralf Palmisano,[10] Enrico Solcia,[3] Vittorio Ricci,[3] and Steffen Backert[1,11,*]

[1]Department of Biology, Division of Microbiology, University of Erlangen-Nuremberg, Erlangen, Germany
[2]Department of Molecular Biology, University of Salzburg, Salzburg, Austria
[3]Pathologic Anatomy and Human Physiology Units and Centro Grandi Strumenti, University of Pavia and Fondazione IRCCS Policlinico San Matteo, Pavia, Italy
[4]Helmholtz Centre for Infection Research, Microscopy Unit, Braunschweig, Germany
[5]Institute of Pathology, University of Erlangen-Nuremberg, Erlangen, Germany
[6]Institute of Pathology, University of Bern, Bern, Switzerland
[7]Paul Ehrlich Institute, Department of Microbiology, Langen, Germany
[8]University of Porto, i3S, IPATIMUP, Faculty of Medicine, Porto, Portugal
[9]Otto von Guericke University, Institute of Experimental Internal Medicine, Magdeburg, Germany
[10]Optical Imaging Centre, University of Erlangen-Nuremberg, Erlangen, Germany
[11]Lead Contact
*Correspondence: steffen.backert@fau.de
https://doi.org/10.1016/j.chom.2017.09.005

SUMMARY

The *Helicobacter pylori* (*Hp*) type IV secretion system (T4SS) forms needle-like pili, whose binding to the integrin-β_1 receptor results in injection of the CagA oncoprotein. However, the apical surface of epithelial cells is exposed to *Hp,* whereas integrins are basolateral receptors. Hence, the mechanism of CagA delivery into polarized gastric epithelial cells remains enigmatic. Here, we demonstrate that T4SS pilus formation during infection of polarized cells occurs predominantly at basolateral membranes, and not at apical sites. *Hp* accomplishes this by secreting another bacterial protein, the serine protease HtrA, which opens cell-to-cell junctions through cleaving epithelial junctional proteins including occludin, claudin-8, and E-cadherin. Using a genetic system expressing a peptide inhibitor, we demonstrate that HtrA activity is necessary for paracellular transmigration of *Hp* across polarized cell monolayers to reach basolateral membranes and inject CagA. The contribution of this unique signaling cascade to *Hp* pathogenesis is discussed.

INTRODUCTION

Type IV secretion systems (T4SSs) are large membrane-associated transporter complexes present in Gram-negative and Gram-positive bacteria as well as in some Archaea. These T4SSs operate in a contact-dependent fashion and are functionally diverse both in terms of the transported substrate (proteins or DNA-protein complexes) and the recipients, which can be either bacteria of the same or different species, or higher organisms such as plants, fungi, or mammalian cells (Gonzalez-Rivera et al., 2016). Bacterial pathogens including *Agrobacterium*, *Helicobacter*, *Legionella*, *Brucella*, and *Bartonella* employ T4SSs to support their survival and proliferation in eukaryotic hosts. The prototypical T4SS is that of *Agrobacterium tumefaciens*, which delivers oncogenic nucleoprotein particles (T-DNA) into plant cells, leading to crown gall tumor growth, while the other T4SSs translocate effector proteins (Backert et al., 2015). T4SSs typically consist of 11 VirB proteins (encoded by *virB1–11* genes) and the so-called coupling protein (VirD4, an ATPase). The agrobacterial VirB proteins can be grouped into three categories: (1) the putative channel or core components (VirB6-10), (2) the energetic components (the NTPases VirB4 and VirB11), and (3) the pilus-associated components (VirB2, VirB3, and VirB5). Structural studies have demonstrated that multiple VirB proteins assemble into 3 megadalton T4SS nanomachines that span the entire cell envelope (Low et al., 2014). This complex comprises an outer membrane-associated core structure connected by a central stalk to a substantial inner membrane assembly composed of 12 VirB4 ATPase subunits arranged as side-by-side hexameric barrels.

The *Hp* T4SS is encoded by the *cag* pathogenicity island (*cag*PAI) and contains up to 32 genes expressing all VirB orthologs and VirD4 as well as several auxiliary factors (Backert et al., 2015). The presence of this T4SS has been associated with several disorders ranging from chronic gastritis to ulceration to gastric cancer (Wroblewski and Peek, 2016). Electron microscopy identified a 41 nm core structure (Frick-Cheng et al., 2016) and the T4SS pilus protruding from the bacterial surface (Kwok et al., 2007). These T4SS pili are induced upon host contact and often locate at one bacterial cell pole. The majority of T4SSs in pathogens do not translocate their effectors into the culture supernatant. This suggests that functional activation of the T4SS requires a signal from the host cell, for example, the interaction with a specific receptor. Host cell integrin-$\alpha_5\beta_1$ was previously shown to directly interact with *Hp* T4SS proteins

and is so far the only T4SS receptor known (Kwok et al., 2007; Kaplan-Türköz et al., 2012; Bonsor et al., 2015). Integrins are transmembrane cell adhesion molecules that mediate cell-to-cell and cell-matrix interactions, anchoring cells to the underlying substratum (Mui et al., 2016), and represent therapeutic targets in various cancers (Blandin et al., 2015). Clustered integrins assemble into actin-rich structures known as focal adhesions, where integrin signaling is mediated (Multhaupt et al., 2016). Binding of T4SS proteins such as CagL and CagY to integrins induces local membrane ruffling and integrin clustering, indicative of a general effect on membrane dynamics, which is the first T4SS activity on host cells (Tegtmeyer et al., 2010). Once the T4SS pilus is established, *Hp* delivers peptidoglycan (Viala et al., 2004), chromosomal DNA (Varga et al., 2016), heptose-1,7-bisphosphate (Stein et al., 2017), and the CagA effector protein, followed by phosphorylation at EPIYA motifs through oncogenic Src and Abl tyrosine kinases (Mueller et al., 2012). However, most of the studies were done with non-polarized AGS cells, where integrins are easily accessible, but the mechanism of CagA translocation in the polarized gastric epithelium remains fully unknown.

In polarized epithelial cells, integrins are generally expressed at basolateral surfaces, being protected by tight junctions (TJs) and E-cadherin-based adherens junctions (AJs). This prompted us to investigate whether *Hp* can establish contact with integrins at the basolateral surface to inject CagA. Here, we demonstrate that *Hp* T4SS pilus formation and CagA delivery into polarized epithelial cells occur at basolateral, and not at apical sites. A second bacterial factor, the secreted serine protease HtrA (Hoy et al., 2010; Schmidt et al., 2016; Tegtmeyer et al., 2016), is required and paves the way for *Hp* by opening the cell-to-cell junctions. This occurs through fragmentation of AJ proteins such as E-cadherin, cleaving off its 90-kDa extracellular domain and proposed cleavage of other yet unknown HtrA targets in the TJs, followed by paracellular transmigration of the bacteria across the polarized cell monolayer. Consequently, we propose a unique model in which *Hp* travels to basolateral membranes and injects CagA in an integrin-dependent manner.

RESULTS

Epithelial Colonization of *Hp* at Cell-to-Cell Junctions, Secretion of HtrA, and Disruption of E-Cadherin in Gastric Biopsies

We have recently demonstrated *in vitro* that *Hp* can secrete the serine protease HtrA into the medium, which cleaves E-cadherin (Hoy et al., 2012). To investigate whether these findings exert *in vivo* relevance in *Hp*-colonized patients, we used transmission electron microscopy (TEM) on biopsy samples taken from the gastric antrum of 20 subjects undergoing routine endoscopic examination for dyspeptic symptoms (Necchi et al., 2007). We tested two different antibodies directed against HtrA, both of which reacted specifically with *Hp* HtrA, but not with other bacterial and host cell proteins on western blots (Figure S1A). Our ultrastructural immunogold procedure by TEM revealed that HtrA-positive *Hp*, besides colonizing the gastric epithelial cells at apical sites *in vivo*, fills deeply penetrating intercellular clefts (Figure 1A), where the HtrA protease is massively secreted (Figures S1B and S1C), and directly contacts profoundly dislocated intercellular TJs (Figures 1A–1C, blue arrowheads). The stainings show both HtrA within the bacteria (violet arrows) and secreted HtrA (yellow arrows) detected in the extracellular environment (Figure S1C). In addition, HtrA was found to penetrate intercellularly at the level of the cell-to-cell junctional system (Figures 1B and 1C, green arrows). As a control, *Hp*-negative gastric biopsy specimens revealed normally preserved TJs, AJs, and desmosomes; no intercellular clefts; and, as expected, no HtrA signals (Figures S1D and S1E).

The expression of E-cadherin is commonly downregulated in gastric cancer (Costa et al., 2013). Next, we employed immunohistochemistry (IHC) to detect the ectodomain of E-cadherin and assessed the *Hp* status in gastric tissues from patients with neoplasia (Figures 1D–1F, S1F, and S1G). Compared to *Hp*-negative atrophic gastritis biopsies with intestinal metaplasia (Figure 1D), we observed decreased epithelial E-cadherin staining in *Hp*-infected mucosa samples (Figure 1E). Quantifying the E-cadherin staining in *Hp*-negative versus *Hp*-positive tissues revealed a statistically significant drop by about 40%, indicating that *Hp* infections are associated with the loss of the E-cadherin ectodomain *in vivo* (Figure 1F). Thus, the large extent of E-cadherin depletion associated with high levels of secreted HtrA resembles a severe disturbance of the mucosal barrier in the *Hp*-infected stomach.

HtrA Cleavage of Occludin and Claudin-8 and *Hp* Transmigration across Polarized Epithelial Cells

In the following experiments, we investigated the interaction of *Hp* with cultured polarized epithelial cells. For this purpose, MDCK, MKN28, and NCI-N87 cells were differentiated for 2 weeks. TEM and field emission scanning electron microscopy (FESEM) identified the presence of apical microvilli (Figures 2A and S1H) and confocal laser scanning microscopy (CLSM) confirmed proper localization of the apical marker protein ezrin (Figure S1I). Similar to our *in vivo* observations described above, FESEM revealed the time-dependent attachment of *Hp* to the apical surface in close proximity to the cell-to-cell junctions after 4 and 8 hr (Figure 2A, yellow dashed lines). This was accompanied by fragmentation of the TJ proteins occludin and claudin-8 during infection (Figure 2B). Both proteins were confirmed as HtrA targets by *in vitro* cleavage using the recombinant proteins (Figures S2A and S2B). CLSM was then used to visualize the bacteria and integrin-β_1 in z stacks taken from apical down to basal sites. As shown in Figure 2C, integrin-β_1 revealed the typical basolateral localization as expected for polarized cells (upper panel, red). To visualize the bacteria, we counterstained the samples using an antibody against *Hp* (lower panel, green). After 24 hr infection, we found *Hp* at apical (white arrows) and transmigrated bacteria at basolateral sites (blue arrows) (Figure 2C). This suggests that *Hp* can efficiently disrupt both the TJs and AJs, and enter cell monolayers after several hours of infection.

T4SS Pilus Formation by *Hp* Occurs at Basolateral and Not Apical Epithelial Surfaces

Having established three useful *in vitro* polarized epithelial cell systems for *Hp* infection, we closely inspected the apically bound bacteria for T4SS pilus formation by FESEM. The results show that the majority of these bacteria exhibited no pili at all,

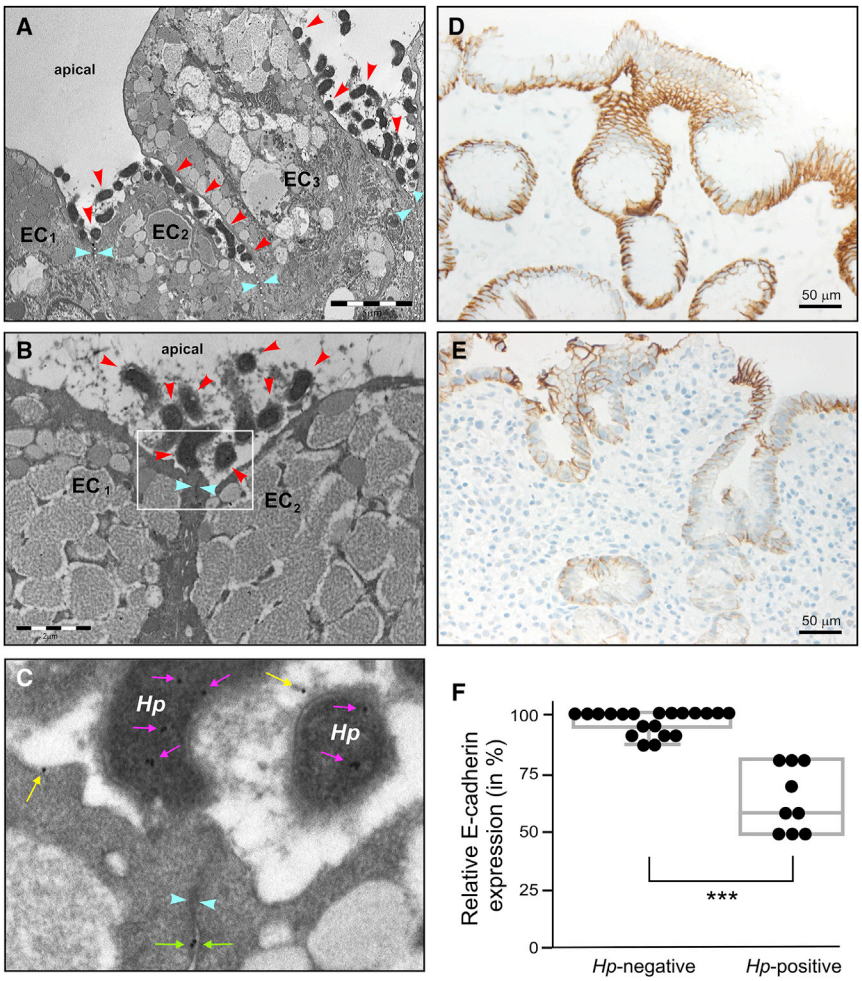

Figure 1. *Hp* Secretes Protease HtrA and Attacks Epithelial Cell-to-Cell Junctions *In Vivo*

(A) TEM of human gastric epithelial cells *in vivo* showing two *Hp*-filled (red arrowheads), deeply penetrating intercellular clefts on both sides of one epithelial cell (EC_3, bulging into the lumen). A normal, non-penetrating, small pit is seen on the left side, between EC_1 and EC_2, closed by a normally situated juxtaluminal junctional complex (blue arrowheads), to be compared with the deeply dislocated junctions closing penetrating clefts.

(B) TEM of two mucus-secreting cells (EC_1 and EC_2) *in vivo* that are colonized by *Hp* (red arrowheads) near the tight junctions (blue arrowheads).

(C) A specific section (white box) is enlarged and exhibits plenty of HtrA immunogold particles on the bacterial bodies (violet arrows) as well as secreted HtrA (yellow arrows) and at the level of the intercellular junctional system (green arrows).

(D and E) Loss of the extracellular E-cadherin domain in *Hp*-colonized tissues. IHC staining of *Hp*-negative tissue (D) and *Hp*-colonized tissues (E). The extracellular E-cadherin domain is labeled and shows a continuous basolateral staining in foveolar epithelia of the antrum (D), which is widely disrupted upon *Hp* infection (E). The *Hp* status in the corresponding tissues was confirmed by IHC (Figures S1F and S1G).

(F) Relative E-cadherin ectodomain staining (maximal intensity in *Hp*-negative samples defined as 100%) in the *Hp*-negative (n = 20) versus *Hp*-positive (n = 9) samples differs significantly (two-tailed Mann-Whitney test, $p < 10^{-4}$).

See also Figure S1.

with only a few having one visible pilus (Figures 3A and 3C). We then removed the cell monolayer from the substratum and investigated the basolateral *Hp*. Strikingly, more than 70% of the transmigrated basolateral bacteria exhibited T4SS pili and up to six pili per bacterium were detected (Figures 3B and 3C). This strongly supports the view that the T4SS is inactive when *Hp* adheres to apical surfaces, but becomes activated after traveling through the epithelial cell monolayer and reaching integrin-rich basolateral compartments.

Intracellular Phosphorylated CagA Co-localizes with Basolateral Integrin-β_1

The above data imply that *Hp* transmigration may be an important pre-requisite for proper T4SS function. To investigate whether the HtrA-induced disruption of cell-to-cell junctions and *Hp* traveling supports CagA translocation into host cells, we analyzed CagA phosphorylation in infected MKN28 monolayers using an antibody recognizing phosphorylated CagA at tyrosine residue 972, also known as EPIYA-motif C. The specificity of the antibody for phospho-CagA-EPIYA-C was confirmed by western blotting (Kwok et al., 2007) and lack of staining in uninfected MKN28 control cells (Figure 3D, upper panel). Remarkably, CLSM of infected cells revealed pronounced phospho-CagA signals co-localizing with integrin-β_1 at basolateral sites, as indicative for translocated CagA (Figure 3D, lower panel, arrows). We also noted that the integrin-β_1 distribution slightly changed during the infection course. Quantification indicated a shift (up to 20%) of the overall integrin-β_1 signal from basal to basolateral sites upon infection (Figure 3D). Taken together, these data indicate that CagA is injected across basolateral-expressed integrin-β_1 after HtrA-mediated opening of cell-to-cell junctions and transmigration of the bacteria.

Expression of HtrA Inhibitory Peptide Abrogates *Hp* Transmigration and CagA Translocation

To corroborate the above findings further, we aimed to mutagenize *htrA*. Since *htrA* is an essential gene in *Hp* and cannot be deleted (Tegtmeyer et al., 2016), we applied the HtrA inhibitor P1, a peptide (TGTLLLI↓LSDVNDNAPIPEPR) derived from a recently identified HtrA cleavage site in E-cadherin (Schmidt et al., 2016). We cloned the P1 sequence under the control of the arabinose-inducible pBAD system (Guzman et al., 1995). To check whether the expression system works in *Hp*, this genetic element was first cloned together with the luciferase gene in the shuttle vector pSB13 (Figure S2C). Transformation of this vector into *Hp* followed by addition of L-arabinose resulted in strong and specific luciferase activation (Figures S2D and S2E). Next, we replaced the luciferase gene by a construct

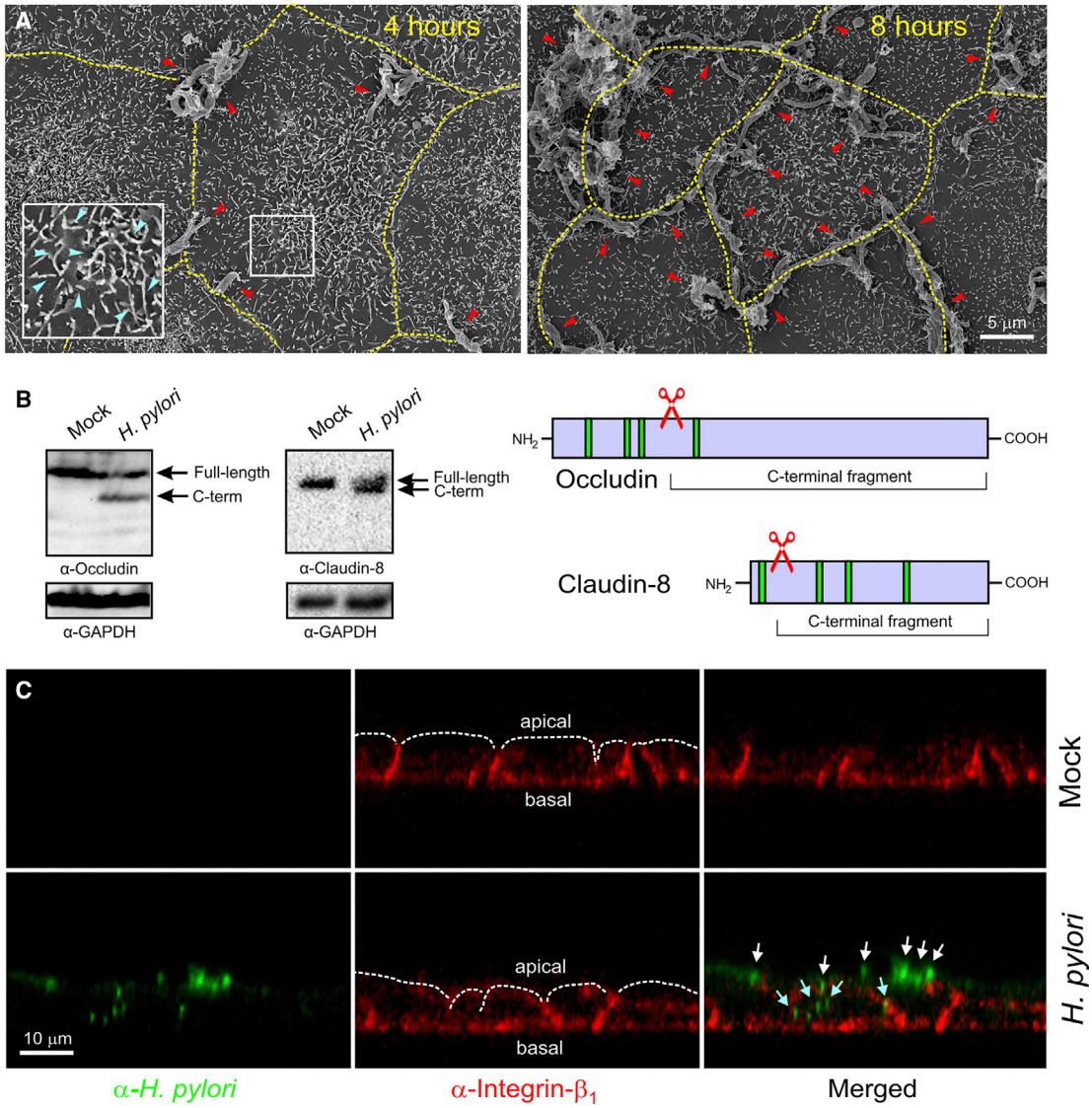

Figure 2. Apical Attachment of *Hp* at the Junctions of Polarized Epithelial Cells, Cleaving of Tight Junction Proteins Occludin and Claudin-8, and Paracellular Transmigration during Infection

(A) Scanning electron microscopy showing time-dependent binding of *Hp* strain P12 (red arrowheads) at the cell-to-cell junctions of infected MDCK cells marked by dashed yellow lines. A specific section (white box) is enlarged and exhibits microvilli (blue arrowheads).

(B) Infection was accompanied by cleavage of occludin and claudin-8 (arrows). Occludin and claudin-8 are shown as bars with indicated positions of transmembrane domains (green) and mapped HtrA cleavage sites in extracellular domains (red).

(C) Confocal microscopy of integrin-β_1 (red) at the membranes of polarized MKN28 cells along the xz axis demonstrated basal and basolateral membrane localization of integrin-β_1 and revealed *Hp* (green) at the apical surface (white arrows) and in the intercellular space between neighboring MKN28 cells (blue arrows) 24 hr post-infection.

See also Figure S2.

expressing the P1 peptide fused to an N-terminal signal sequence and C-terminal hemagglutinin (HA)-tag for antibody detection (Figure S2F, top). Our results show that P1 can be induced by L-arabinose in a dose-dependent manner and upregulation of P1 expression in *Hp* resulted in dose-dependent inhibition of HtrA activity as determined by casein zymography (Figure 3E). As further controls, the expression of HtrA and other well-known *Hp* virulence proteins, including GGT, VacA, CagA, and UreB, remained unaffected (Figure S2G). Infection of polarized MKN28 cells with P1-expressing *Hp* in the presence of L-arabinose resulted in a significant downregulation of bacterial transmigration as compared to the non-treated control (Figure 3F). This result was confirmed by TEM of infected MKN28 samples showing that paracellular transmigration of *Hp* appears and can be blocked by expression of P1 (Figures 4A and 4B). This phenotype nicely correlated with the abrogation of L-arabinose-dependent HtrA protease activity as well as CagA translocation and phosphorylation in the same time course

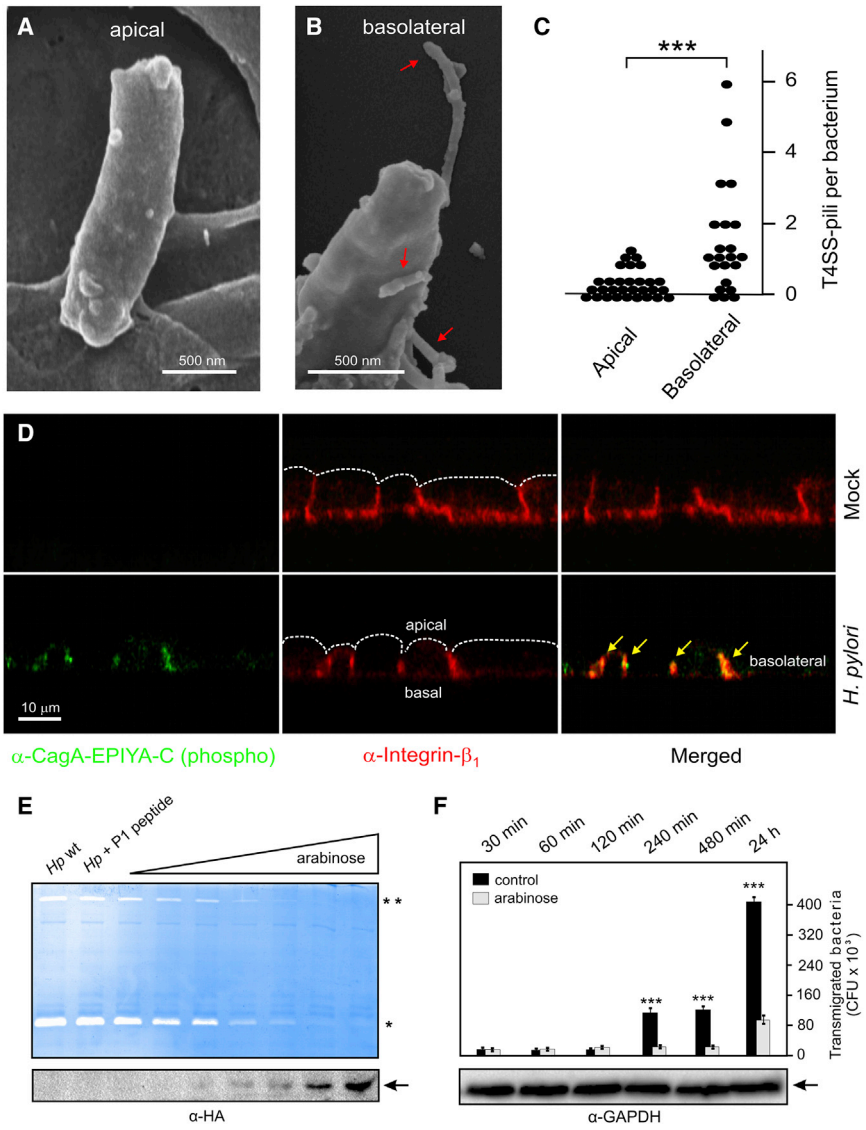

Figure 3. Basolateral Activation of T4SS Pili and Detection of Translocated CagA upon HtrA-Dependent Transmigration of *Hp*

(A) Scanning electron microscopy of top views shows apically attached *Hp* strain P12 with no T4SS pili present.

(B) Investigation of basolateral bacteria revealed multiple T4SS pili (red arrows).

(C) Quantification of T4SS pili exposed by apical and basal *Hp*.

(D) Phosphorylation of translocated CagA (green) and localization of integrin-β_1 (red) were examined in polarized MKN28 cells after infection with *Hp* for 24 hr by confocal microscopy along the xz axis. Staining with a phosphospecific antibody revealed basolateral co-localization of phospho-CagA with integrin-β_1 in infected cells (yellow arrows). Mock control cells revealed no phospho-CagA signals as expected.

(E) The HtrA inhibitory peptide P1 (HA-tagged) was cloned under the control of the arabinose-inducible pBAD promotor in *Hp* strain B8. Addition of L-arabinose resulted in strong, specific, and dose-dependent P1 expression and HtrA inhibition as indicated by western blotting and casein zymography. Asterisks indicate the position of proteolytic active HtrA monomers (*) and oligomers (**) on the gel.

(F) Infection of polarized MKN28 cells in the transwell system with P1-expressing *Hp* in the presence of L-arabinose resulted in a significant downregulation of bacterial transmigration as compared to the non-treated control.

Data are represented as mean ± SEM. See also Figure S3.

(Figures 4C, 4D, and S3A–S3D). As controls, cell binding of *Hp* and induction of interleukin-8 (IL-8) were not affected by P1 expression (Figures S3E and S3F). These findings strongly support the hypothesis that proteolytic activity of HtrA is critically required for bacterial transmigration and translocation and phosphorylation of CagA, but not for signaling leading to IL-8 secretion.

Stable Expression of E-Cadherin in AGS Changes Cell Polarity and CagA Translocation

To corroborate the above findings further, we aimed to compare CagA translocation and phosphorylation in non-polarized versus polarized epithelial cells in the same genetic background. Non-polarized AGS cells do not express E-cadherin; however, stable transduction of the *E-cadherin* gene resulted in a polarized phenotype (Figures S4A and S4B). Infection of E-cadherin-deficient AGS cells with P1 peptide-expressing *Hp* in the presence of L-arabinose led to efficient CagA translocation and phosphorylation over time (Figures S4C and S4G), but not in E-cadherin-expressing AGS cells under the same conditions (Figures S4D and S4H). As expected, CagA can be similarly well phosphorylated in both cell lines in the absence of arabinose, but with a notable delay in E-cadherin-expressing AGS cells (Figures S4E–S4H). Based on the above functional studies, we could therefore demonstrate that HtrA activity is required for translocation and phosphorylation of CagA in infected E-cadherin-expressing polarized cells, but not in non-polarized control cells. Thus, HtrA and T4SS functions work together cooperatively during infection of polarized gastric epithelial cells and lead to basolateral delivery and phosphorylation of CagA.

DISCUSSION

The pathogen and type I carcinogen *Hp* infects about half of the human world population and is associated with severe gastric diseases. Here, we report on a unique mechanism of integrin receptor-dependent T4SS activation during infection of polarized gastric epithelial cells (summarized in Figure 4E). It is well established that *Hp* translocates the virulence factor CagA into the host cell cytoplasm, where it can interact with an array of ~24 known host signaling proteins in phosphorylation-dependent and phosphorylation-independent manners, manipulating

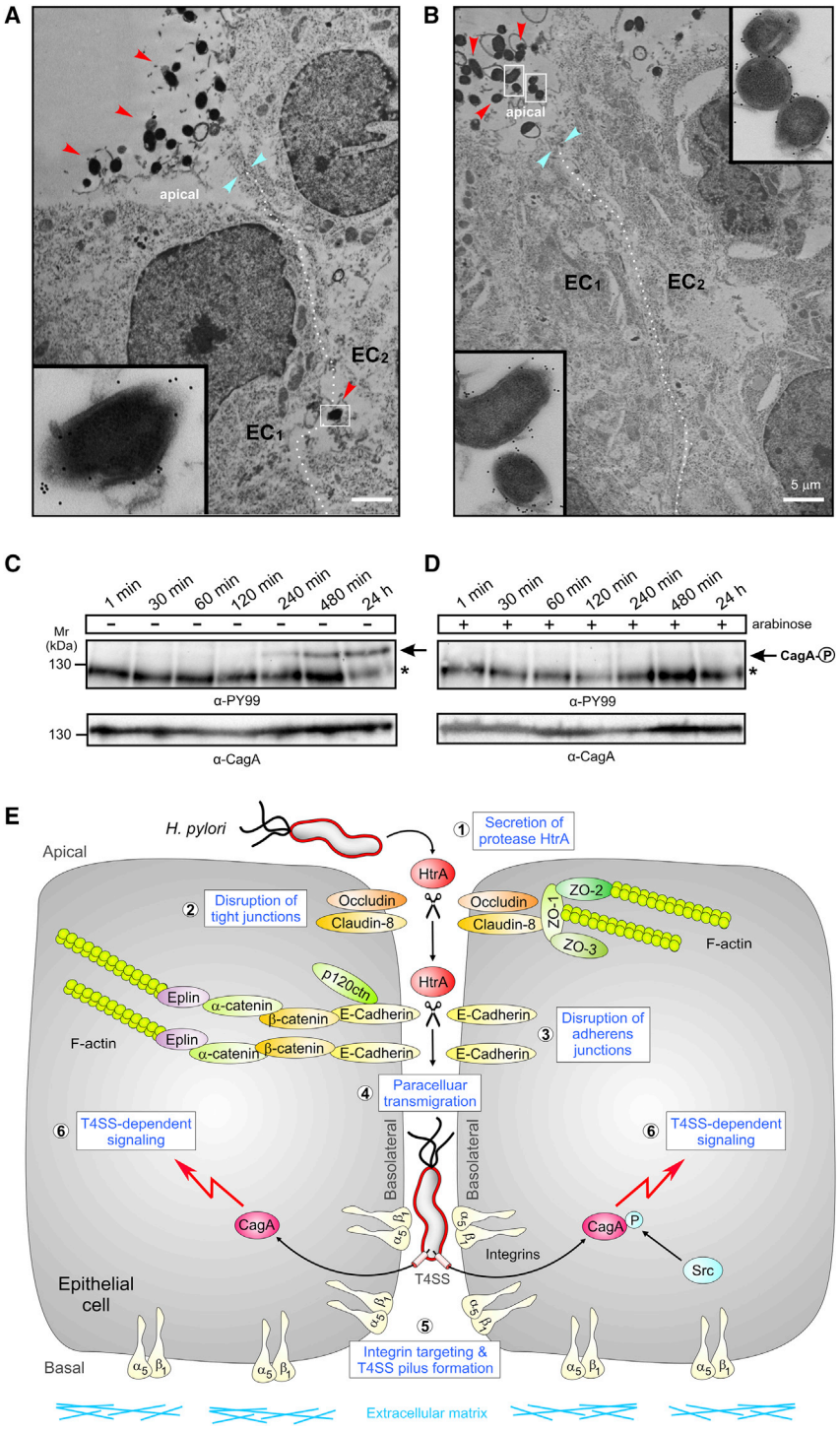

Figure 4. Translocation and Phosphorylation of CagA in Polarized Cells Require HtrA Protease Activity

(A and B) Differentiated monolayers of MKN28 cells were infected with wild-type *Hp* strain B8 (A) or a P1 peptide-expressing mutant (B).

(A) TEM shows a bacterium deeply penetrated into the intercellular space (dotted line), enlarged in the inset to show its *Hp*-specific α-VacA staining.

(B) No bacterial penetration into the intercellular space was detected. The insets show immunoreactivity of the luminal bacteria for VacA. Red arrowheads indicate similar high numbers of bound *Hp* bacteria and blue arrowheads show tight junctions.

(C) In the absence of arabinose, P1-encoding *Hp* exhibits strong HtrA protease activity (compare with Figure S3) and translocates CagA followed by phosphorylation.

(D) In the presence of arabinose, P1-expressing *Hp* displays decreasing HtrA protease activity (compare with Figure S3), which correlates with abrogation of CagA translocation and phosphorylation as shown here. Arrows indicate the position of phospho-CagA on the gels and asterisks the position of a phosphorylated 125-kDa host cell protein.

(E) Model for the role of *Hp* HtrA in type IV secretion of CagA into polarized epithelial cells. The current data indicate that the pathogen uses a paracellular transmigration route to reach its T4SS host cell receptor, integrin-β_1, at basolateral surfaces as indicated. For this purpose, HtrA targets specific host cell factors in the TJs (occludin and claudin-8) and AJs (E-cadherin), and may hijack indicated host cell signaling cascades. We defined six subsequent steps involved in this process as shown. For more details, see text.

See also Figure S4.

fundamental processes in the gastric epithelium, including cell adhesion, polarity, proliferation, and actin-cytoskeletal rearrangements (Backert et al., 2015). Among them are various cancer-associated signal transduction pathways, including β-catenin engagement (Franco et al., 2005; Murata-Kamiya et al., 2007) and Snail-mediated epithelial-mesenchymal transition (Lee et al., 2014). Previously, it was also shown that *Hp* interacts with the apical junctional complex (Amieva et al., 2003; Wroblewski et al., 2015) and we described integrin-β_1 as receptor for CagA translocation (Kwok et al., 2007). However, it remained unclear how *Hp* can target basolateral-expressed integrin-β_1 when lateral cell-to-cell adhesions are still intact in polarized epithelial cells. In fact, we identified HtrA as a secreted bacterial serine protease *in vitro* and *in vivo* that directly targets the TJ proteins occludin and claudin-8 as well as the AJ factor E-cadherin in polarized gastric epithelial cells. E-cadherin ectodomain shedding upon *Hp* infection has been confirmed previously in two polarized cell models (MCF-7 and NCI-N87) and did not require a functional T4SS or CagA (Weydig et al., 2007; Schirrmeister et al., 2009). These findings are in line with observations that infected patients exhibited significantly higher serum levels of soluble E-cadherin than uninfected controls, which was independent of the CagA status in the *Hp* strain (O'Connor et al., 2011). Besides the role of HtrA as shown in the present paper, differences of methylation

patterns or somatic mutations in the *E-cadherin* gene might further affect E-cadherin function in gastric carcinomas (Costa et al., 2013). Since TJ and AJ complexes are intimately connected to the intracellular cytoskeleton (Figure 4E), HtrA-mediated cleavage of junctional proteins can disrupt cell-to-cell adhesions and induce the disintegration of epithelial barrier functions, which can also explain the occurrence of deep epithelial clefts in the colonized gastric epithelium *in vivo* (Figures 1A and S1B). After these cleavage events, *Hp* can efficiently enter the intercellular space between neighboring cells, allowing travel to basolateral surfaces and CagA translocation across integrin-β_1. In conjunction with these findings, we provide evidence that pilus formation and thereby activation of the T4SS mainly occurs at basolateral sites (Figure 4E). Finally, we established an inducible inhibitory peptide expression system in *Hp*, which profoundly blocks HtrA activity and CagA injection. Altogether, HtrA-dependent opening of cell-to-cell junctions and T4SS activation represent an innovative strategy allowing persistent *Hp* colonization and pathogenicity. Finally, our present data also indicate that the induction of pro-inflammatory IL-8 secretion by the bacteria may proceed independently of HtrA and integrins, which should be investigated in more detail in future studies. It will also be interesting to study whether additional HtrA-expressing pathogens use a similar infection strategy to break the epithelial barrier in other niches of the human body.

STAR★METHODS

Detailed methods are provided in the online version of this paper and include the following:

- KEY RESOURCES TABLE
- CONTACT FOR REAGENT AND RESOURCE SHARING
- EXPERIMENTAL MODEL AND SUBJECT DETAILS
  - Commercial Cell Lines and Infection Experiments
  - Microbes
- METHOD DETAILS
  - Bacterial Mutagenesis
  - Construction of E-Cadherin-Expressing AGS Cells
  - Quantification of IL-8 Cytokines by ELISA
  - TER Measurement and Transwell Infection Studies
  - *In vitro* Cleavage Assays of Occludin and Claudin-8 by HtrA
  - Bacterial Cell Binding Assay
  - Cloning and Purification of Recombinant HtrA Protein
  - Casein Zymography
  - Antibodies
  - Transmission Electron Microscopy (TEM) and Immunogold Labeling Studies
  - Field Emission Scanning Electron Microscopy (FESEM)
  - Immunohistochemistry (IHC)
  - Immunofluorescence Staining and Confocal Laser Scanning Microscopy (CLSM)
  - SDS-PAGE and Immunoblotting
- QUANTIFICATION AND STATISTICAL ANALYSIS
  - Quantitation of Signals in Western Blots and Casein Gels
  - Statistics

SUPPLEMENTAL INFORMATION

Supplemental Information includes four figures and can be found with this article online at https://doi.org/10.1016/j.chom.2017.09.005.

AUTHOR CONTRIBUTIONS

All authors commented on the different stages of the work, and read and approved the final manuscript. N.T., S.W., and S.B. conceptualized the study. N.T. performed most of the cloning, mutagenesis, and infection experiments. V.N., M.R., V.R., E.S., and C.I.A. carried out the FESEM and TEM studies. S.W., M.N., and R.P. performed and analyzed the CLSM experiments and T.T.R. the IHC stainings. A.H. ran the casein gels and M.B. the transwell studies. H.L. originally investigated the functionality of the arabinose-inducible pBAD promotor in *Hp* and performed luciferase assays. C.F. provided the *E-cadherin*-expressing AGS cells. S.B. wrote the manuscript. N.T., S.W., V.R., and E.S. reviewed and edited the final version of the paper.

ACKNOWLEDGEMENTS

We thank Christiane Weydig and Wilhelm Brill for technical assistance, and Dr. Timothy Cover for the α-VacA antibody. This work is supported by a grant of the German Science Foundation (DFG) to S.B. (project A04 in CRC-1181). N.T. was supported by DFG grant TE776/3-1 and S.W. by grant P-24074 from Austrian Science Fund (FWF). The work of E.S. and V.R. was funded by Fondazione Cariplo (Milan, Italy; grants 2009-2532 and 2011-0485, respectively). C.F. is supported by the North Portugal Regional Operational Programme (NORTE-01-0145-FEDER-000029).

Received: March 22, 2017
Revised: July 26, 2017
Accepted: September 8, 2017
Published: October 11, 2017

REFERENCES

Amieva, M.R., Vogelmann, R., Covacci, A., Tompkins, L.S., Nelson, W.J., and Falkow, S. (2003). Disruption of the epithelial apical-junctional complex by Helicobacter pylori CagA. Science *300*, 1430–1434.

Backert, S., Kwok, T., and König, W. (2005). Conjugative plasmid DNA transfer in *Helicobacter pylori* mediated by chromosomally encoded relaxase and TraG-like proteins. Microbiology *151*, 3493–3503.

Backert, S., Tegtmeyer, N., and Fischer, W. (2015). Composition, structure and function of the *Helicobacter pylori cag* pathogenicity island encoded type IV secretion system. Future Microbiol. *10*, 955–965.

Blandin, A.F., Renner, G., Lehmann, M., Lelong-Rebel, I., Martin, S., and Dontenwill, M. (2015). β1 integrins as therapeutic targets to disrupt hallmarks of cancer. Front. Pharmacol. *6*, 279.

Boehm, M., Hoy, B., Rohde, M., Tegtmeyer, N., Bæk, K.T., Oyarzabal, O.A., Brøndsted, L., Wessler, S., and Backert, S. (2012). Rapid paracellular transmigration of *Campylobacter jejuni* across polarized epithelial cells without affecting TER: role of proteolytic-active HtrA cleaving E-cadherin but not fibronectin. Gut Pathog. *4*, 3.

Boehm, M., Lind, J., Backert, S., and Tegtmeyer, N. (2015). *Campylobacter jejuni* serine protease HtrA plays an important role in heat tolerance, oxygen resistance, host cell adhesion, invasion, and transmigration. Eur. J. Microbiol. Immunol. (Bp.) *5*, 68–80.

Bonsor, D.A., Pham, K.T., Beadenkopf, R., Diederichs, K., Haas, R., Beckett, D., Fischer, W., and Sundberg, E.J. (2015). Integrin engagement by the helical RGD motif of the Helicobacter pylori CagL protein is regulated by pH-induced displacement of a neighboring helix. J. Biol. Chem. *290*, 12929–12940.

Conradi, J., Tegtmeyer, N., Woźna, M., Wissbrock, M., Michalek, C., Gagell, C., Cover, T.L., Frank, R., Sewald, N., and Backert, S. (2012). An RGD helper sequence in CagL of *Helicobacter pylori* assists in interactions with integrins and injection of CagA. Front. Cell. Infect. Microbiol. *2*, 70.

Costa, A.M., Leite, M., Seruca, R., and Figueiredo, C. (2013). Adherens junctions as targets of microorganisms: a focus on Helicobacter pylori. FEBS Lett. *587*, 259–265.

Crull, K., Rohde, M., Westphal, K., Loessner, H., Wolf, K., Felipe-López, A., Hensel, M., and Weiss, S. (2011). Biofilm formation by Salmonella enterica serovar Typhimurium colonizing solid tumours. Cell. Microbiol. *13*, 1223–1233.

Farnbacher, M., Jahns, T., Willrodt, D., Daniel, R., Haas, R., Goesmann, A., Kurtz, S., and Rieder, G. (2010). Sequencing, annotation, and comparative genome analysis of the gerbil-adapted *Helicobacter pylori* strain B8. BMC Genomics *11*, 335.

Fischer, W., Windhager, L., Rohrer, S., Zeiller, M., Karnholz, A., Hoffmann, R., Zimmer, R., and Haas, R. (2010). Strain-specific genes of *Helicobacter pylori:* genome evolution driven by a novel type IV secretion system and genomic island transfer. Nucleic Acids Res. *38*, 6089–6101.

Franco, A.T., Israel, D.A., Washington, M.K., Krishna, U., Fox, J.G., Rogers, A.B., Neish, A.S., Collier-Hyams, L., Perez-Perez, G.I., Hatakeyama, M., et al. (2005). Activation of beta-catenin by carcinogenic Helicobacter pylori. Proc. Natl. Acad. Sci. USA *102*, 10646–10651.

Frick-Cheng, A.E., Pyburn, T.M., Voss, B.J., McDonald, W.H., Ohi, M.D., and Cover, T.L. (2016). Molecular and structural analysis of the Helicobacter pylori cag type IV secretion system core complex. MBio *7*, e02001–e02015.

Gonzalez-Rivera, C., Bhatty, M., and Christie, P.J. (2016). Mechanism and function of type IV secretion during infection of the human host. Microbiol. Spectr. *4*, https://doi.org/10.1128/microbiolspec.VMBF-0024-2015.

Guzman, L.M., Belin, D., Carson, M.J., and Beckwith, J. (1995). Tight regulation, modulation, and high-level expression by vectors containing the arabinose PBAD promoter. J. Bacteriol. *177*, 4121–4130.

Hoy, B., Löwer, M., Weydig, C., Carra, G., Tegtmeyer, N., Geppert, T., Schröder, P., Sewald, N., Backert, S., Schneider, G., and Wessler, S. (2010). *Helicobacter pylori* HtrA is a new secreted virulence factor that cleaves E-cadherin to disrupt intercellular adhesion. EMBO Rep. *11*, 798–804.

Hoy, B., Geppert, T., Boehm, M., Reisen, F., Plattner, P., Gadermaier, G., Sewald, N., Ferreira, F., Briza, P., Schneider, G., et al. (2012). Distinct roles of secreted HtrA proteases from gram-negative pathogens in cleaving the junctional protein and tumor suppressor E-cadherin. J. Biol. Chem. *287*, 10115–10120.

Kaplan-Türköz, B., Jiménez-Soto, L.F., Dian, C., Ertl, C., Remaut, H., Louche, A., Tosi, T., Haas, R., and Terradot, L. (2012). Structural insights into Helicobacter pylori oncoprotein CagA interaction with β1 integrin. Proc. Natl. Acad. Sci. USA *109*, 14640–14645.

Kwok, T., Backert, S., Schwarz, H., Berger, J., and Meyer, T.F. (2002). Specific entry of *Helicobacter pylori* into cultured gastric epithelial cells via a zipper-like mechanism. Infect. Immun. *70*, 2108–2120.

Kwok, T., Zabler, D., Urman, S., Rohde, M., Hartig, R., Wessler, S., Misselwitz, R., Berger, J., Sewald, N., König, W., and Backert, S. (2007). *Helicobacter* exploits integrin for type IV secretion and kinase activation. Nature *449*, 862–866.

Lee, D.G., Kim, H.S., Lee, Y.S., Kim, S., Cha, S.Y., Ota, I., Kim, N.H., Cha, Y.H., Yang, D.H., Lee, Y., et al. (2014). Helicobacter pylori CagA promotes Snail-mediated epithelial-mesenchymal transition by reducing GSK-3 activity. Nat. Commun. *5*, 4423.

Lind, J., Backert, S., Pfleiderer, K., Berg, D.E., Yamaoka, Y., Sticht, H., and Tegtmeyer, N. (2014). Systematic analysis of phosphotyrosine antibodies recognizing single phosphorylated EPIYA-motifs in CagA of Western-type *Helicobacter pylori* strains. PLoS One *9*, e96488.

Loessner, H., Endmann, A., Leschner, S., Westphal, K., Rohde, M., Miloud, T., Hämmerling, G., Neuhaus, K., and Weiss, S. (2007). Remote control of tumour-targeted *Salmonella enterica* serovar Typhimurium by the use of L-arabinose as inducer of bacterial gene expression *in vivo*. Cell. Microbiol. *9*, 1529–1537.

Low, H.H., Gubellini, F., Rivera-Calzada, A., Braun, N., Connery, S., Dujeancourt, A., Lu, F., Redzej, A., Fronzes, R., Orlova, E.V., and Waksman, G. (2014). Structure of a type IV secretion system. Nature *508*, 550–553.

Mueller, D., Tegtmeyer, N., Brandt, S., Yamaoka, Y., De Poire, E., Sgouras, D., Wessler, S., Torres, J., Smolka, A., and Backert, S. (2012). c-Src and c-Abl kinases control hierarchic phosphorylation and function of the CagA effector protein in Western and East Asian *Helicobacter pylori* strains. J. Clin. Invest. *122*, 1553–1566.

Mui, K.L., Chen, C.S., and Assoian, R.K. (2016). The mechanical regulation of integrin-cadherin crosstalk organizes cells, signaling and forces. J. Cell Sci. *129*, 1093–1100.

Multhaupt, H.A., Leitinger, B., Gullberg, D., and Couchman, J.R. (2016). Extracellular matrix component signaling in cancer. Adv. Drug Deliv. Rev. *97*, 28–40.

Murata-Kamiya, N., Kurashima, Y., Teishikata, Y., Saito, Y., Higashi, H., Aburatani, H., Akiyama, T., Peek, R.M., Jr., Azuma, T., et al. (2007). Helicobacter pylori CagA interacts with E-cadherin and deregulates the beta-catenin signal that promotes intestinal transdifferentiation in gastric epithelial cells. Oncogene *26*, 4617–4626.

Necchi, V., Candusso, M.E., Tava, F., Luinetti, O., Ventura, U., Fiocca, R., Ricci, V., and Solcia, E. (2007). Intracellular, intercellular, and stromal invasion of gastric mucosa, preneoplastic lesions, and cancer by Helicobacter pylori. Gastroenterology *132*, 1009–1023.

O'Connor, P.M., Lapointe, T.K., Jackson, S., Beck, P.L., Jones, N.L., and Buret, A.G. (2011). Helicobacter pylori activates calpain via toll-like receptor 2 to disrupt adherens junctions in human gastric epithelial cells. Infect. Immun. *279*, 3887–3894.

Oliveira, M.J., Costa, A.M., Costa, A.C., Ferreira, R.M., Machado, J.C., Mareel, M., and Figueiredo, C. (2009). CagA associates with c-Met, E-cadherin, and p120-catenin in a multiproteic complex that suppresses *Hp*-induced cell-invasive phenotype. J. Infect. Dis. *200*, 745–755.

Schindelin, J., Rueden, C.T., Hiner, M.C., and Eliceiri, K.W. (2015). The ImageJ ecosystem: an open platform for biomedical image analysis. Mol. Reprod. Dev. *82*, 518–529.

Schirrmeister, W., Gnad, T., Wex, T., Wolke, C., Naumann, M., and Lendeckel, U. (2009). Ectodomain shedding of E-cadherin and c-Met is induced by Helicobacter pylori infection. Exp. Cell Res. *315*, 3500–3508.

Schmidt, T.P., Perna, A.M., Fugmann, T., Böhm, M., Jan Hiss, Haller, S., Götz, C., Tegtmeyer, N., Hoy, B., Rau, T.T., et al. (2016). Identification of E-cadherin signature motifs functioning as cleavage sites for *Helicobacter pylori* HtrA. Sci. Rep. *6*, 23264.

Snoek-van Beurden, P.A., and Von den Hoff, J.W. (2005). Zymographic techniques for the analysis of matrix metalloproteinases and their inhibitors. Biotechniques *38*, 73–83.

Stein, S.C., Faber, E., Bats, S.H., Murillo, T., Speidel, Y., Coombs, N., and Josenhans, C. (2017). Helicobacter pylori modulates host cell responses by CagT4SS-dependent translocation of an intermediate metabolite of LPS inner core heptose biosynthesis. PLoS Pathog. *13*, e1006514.

Tegtmeyer, N., Hartig, R., Delahay, R.M., Rohde, M., Brandt, S., Conradi, J., Takahashi, S., Smolka, A.J., Sewald, N., and Backert, S. (2010). A small fibronectin-mimicking protein from bacteria induces cell spreading and focal adhesion formation. J. Biol. Chem. *285*, 23515–23526.

Tegtmeyer, N., Wittelsberger, R., Hartig, R., Wessler, S., Martinez-Quiles, N., and Backert, S. (2011). Serine phosphorylation of cortactin controls focal adhesion kinase activity and cell scattering induced by *Helicobacter pylori*. Cell Host Microbe *9*, 520–531.

Tegtmeyer, N., Rivas Traverso, F., Rohde, M., Oyarzabal, O.A., Lehn, N., Schneider-Brachert, W., Ferrero, R.L., Fox, J.G., Berg, D.E., and Backert, S. (2013). Electron microscopic, genetic and protein expression analyses of *Helicobacter acinonychis* strains from a Bengal tiger. PLoS One *8*, e71220.

Tegtmeyer, N., Moodley, Y., Yamaoka, Y., Pernitzsch, S.R., Schmidt, V., Traverso, F.R., Schmidt, T.P., Rad, R., Yeoh, K.G., Bow, H., et al. (2016). Characterisation of worldwide *Helicobacter pylori* strains reveals genetic conservation and essentiality of serine protease HtrA. Mol. Microbiol. *99*, 925–944.

Varga, M.G., Shaffer, C.L., Sierra, J.C., Suarez, G., Piazuelo, M.B., Whitaker, M.E., Romero-Gallo, J., Krishna, U.S., Delgado, A., Gomez, M.A., et al. (2016). Pathogenic Helicobacter pylori strains translocate DNA and activate TLR9 via the cancer-associated cag type IV secretion system. Oncogene *35*, 6262–6269.

Viala, J., Chaput, C., Boneca, I.G., Cardona, A., Girardin, S.E., Moran, A.P., Athman, R., Mémet, S., Huerre, M.R., Coyle, A.J., et al. (2004). Nod1 responds to peptidoglycan delivered by the Helicobacter pylori cag pathogenicity island. Nat. Immunol. *5*, 1166–1174.

Weydig, C., Starzinski-Powitz, A., Carra, G., Löwer, J., and Wessler, S. (2007). CagA-independent disruption of adherence junction complexes involves E-cadherin shedding and implies multiple steps in Helicobacter pylori pathogenicity. Exp. Cell Res. *313*, 3459–3471.

Wiedemann, T., Hofbaur, S., Tegtmeyer, N., Huber, S., Sewald, N., Wessler, S., Backert, S., and Rieder, G. (2012). *Helicobacter pylori* CagL dependent induction of gastrin expression via a novel αvβ5-integrin-integrin linked kinase signalling complex. Gut *61*, 986–996.

Wroblewski, L.E., and Peek, R.M., Jr. (2016). Helicobacter pylori: pathogenic enablers—toxic relationships in the stomach. Nat. Rev. Gastroenterol. Hepatol. *13*, 317–318.

Wroblewski, L.E., Piazuelo, M.B., Chaturvedi, R., Schumacher, M., Aihara, E., Feng, R., Noto, J.M., Delgado, A., Israel, D.A., Zavros, Y., et al. (2015). Helicobacter pylori targets cancer-associated apical-junctional constituents in gastroids and gastric epithelial cells. Gut *64*, 720–730.

Zhang, X.S., Tegtmeyer, N., Traube, L., Jindal, S., Perez-Perez, G., Sticht, H., Backert, S., and Blaser, M.J. (2015). A specific A/T polymorphism in Western tyrosine phosphorylation B-motifs regulates *Helicobacter pylori* CagA epithelial cell interactions. PLoS Pathog. *11*, e1004621.

STAR★METHODS

KEY RESOURCES TABLE

REAGENT or RESOURCE	SOURCE	IDENTIFIER
Antibodies		
Mouse monoclonal anti-AIIB2 integrin-β1	Developmental Studies Hybridoma Bank	Cat#AB_528306; RRID: AB_528306
Mouse monoclonal anti-CagA	Austral Biologicals	Cat#HPM-5001-5; RRID: AB_10890224
Mouse monoclonal pan-phosphotyrosine anti-PY99	Santa Cruz	Cat# sc-7020; RRID: AB_628123
Mouse monoclonal anti-E-cadherin	BD Biosciences	Cat#610182; RRID: AB_397581
Rabbit polyclonal anti-ezrin	Santa Cruz	Cat#sc-6409; RRID: AB_640302
Rabbit polyclonal anti-claudin-8	Thermo Scientific	Cat#42-2400; RRID: AB_2533516
Rabbit polyclonal anti-occludin	Thermo Scientific	Cat#710222; RRID: AB_2532634
Rabbit polyclonal anti-H. pylori	Dako	Cat#B0471
Rabbit polyclonal anti-E-cadherin	Santa Cruz	Cat#sc-7870; RRID: AB_2076666
Rabbit polyclonal anti-HA	Sigma-Aldrich	Cat#H6908; RRID: AB_260070
Rabbit anti-CagA	Austral Biologicals	HPP-5003-9; RRID: AB_10920428
Rabbit polyclonal anti-UreB	Tegtmeyer et al., 2013	N/A
Rabbit polylonal anti-GGT	Tegtmeyer et al., 2013	N/A
Rabbit polyclonal anti-VacA #123	Dr. T.L. Cover (Nashville, TN/USA)	N/A
Rabbit polyclonal anti-HtrA #1578	This study	N/A
Rabbit polyclonal anti-HtrA #20555	This study	N/A
Rabbit polyclonal anti-CagA-EPIYA-C (phospho-specific)	Kwok et al., 2007	N/A
Rabbit polyclonal anti-CagA-EPIYA-C (non-phospho-specific)	Kwok et al., 2007	N/A
Bacterial and Virus Strains		
Helicobacter pylori B8	Farnbacher et al., 2010	N/A
Helicobacter pylori P12	Fischer et al., 2010	N/A
Chemicals, Peptides, and Recombinant Proteins		
SYTO-59	Thermo Scientific	Cat#S11341
Recombinant human occludin	Abnova	Cat#H00004950-P01
Recombinant human claudin-8	Abnova	Cat#H00009073-P01
Recombinant *H. pylori* HtrA (26695)	Boehm et al., 2012	N/A
21 amino acid peptide inhibitor P1 (TGTLLLILSDVNDNAPIPEPR)	Schmidt et al., 2016	N/A
Critical Commercial Assays		
Human IL-8 ELISA Set	Becton Dickinson	Cat#555244
Experimental Models: Cell Lines		
AGS	ECACC	Cat#89090402; RRID: CVCL_0139
MKN28	JCRB	Cat#0253; RRID: CVCL_1416
MDCK	ATCC	Cat#CCL-34; RRID: CVCL_0422
NCI-N87	ATCC	Cat#CRL-5822; RRID: CVCL_1603
Recombinant DNA		
Plasmid: pSB13	Backert et al., 2005	N/A
Plasmid: pSB13luci	This study	N/A
Plasmid: pSB13PBADluci	This study	N/A
Plasmid: pCBGr99-basic	Promega	N/A
Plasmid: pHL222	Loessner et al., 2007	N/A
Plasmid: pHL259	Loessner et al., 2007	N/A
pLenti6/V5 construct expressing the human wild-type E-cadherin cDNA	Oliveira et al., 2009	N/A

(*Continued on next page*)

Continued

REAGENT or RESOURCE	SOURCE	IDENTIFIER
Software and Algorithms		
Huygens Professional Software (version 17.04)	Scientific Volume Imaging	https://svi.nl/Huygens-Professional
Fiji/ImageJ2 (version 2.0.0-rc-43/1.51)	Schindelin et al., 2015	RRID: SCR_002285
Living Image 4.1 software	PerkinElmer	RRID: SCR_014247

CONTACT FOR REAGENT AND RESOURCE SHARING

Further information and requests for resources and reagents should be directed to and will be fulfilled by the Lead Contact, Steffen Backert (steffen.backert@fau.de).

EXPERIMENTAL MODEL AND SUBJECT DETAILS

Commercial Cell Lines and Infection Experiments

The human gastric epithelial cell line AGS is E-cadherin-negative (ECACC, #89090402). E-cadherin-positive MKN28 cells (JCRB, #0253) were frequently used to study E-cadherin-dependent processes (Hoy et al., 2010). MDCK (ATCC, #CCL-34) and NCI-N87 (ATCC, CRL-5822) cells represent other standard model systems to study cell-to-cell junctions. All cell lines were grown on 6-well plates in RPMI1640 medium containing 4 mM glutamine (Invitrogen), and 10% FCS (Sigma) in a humidified atmosphere at 37°C. *Helicobacter pylori* (*Hp*) wild-type strains P12 and B8 were cultured as described and cells were infected at a multiplicity of infection (MOI) of 25 (Wiedemann et al., 2012).

Microbes

Hp strain B8 and its mutants were grown on horse serum GC agar plates, supplemented with vancomycin (10 μg/ mL), nystatin (1 μg/mL) and trimethoprim (5 μg/mL), at 37°C for 2 days in anaerobic jars containing a CampyGen gas mix (Oxoid) (Wiedemann et al., 2012). *Hp* grown on agar plates was harvested and resuspended in Phosphate Buffered Saline (PBS, pH 7.4) using sterile cotton swabs (Carl Roth). The bacterial concentration was measured as optical density (OD) at 550 nm using an Eppendorf spectrophotometer.

METHOD DETAILS

Bacterial Mutagenesis

Using the *E. coli-Hp* shuttle plasmid pSB13 as backbone (Backert et al., 2005), an L-arabinose inducible expression construct for firefly luciferase was constructed. The gene encoding the firefly luciferase variant CBGr99 (*luc*) was obtained from plasmid pCBGr99-basic (Promega) by cleavage with *Nco*I and *Hpa*I. This fragment was inserted into plasmid pHL222 (Loessner et al., 2007) at the *Nco*I site and the blunted *Hind*III site, giving rise to plasmid pHL310. Via *Xba*I restriction, *luc* was obtained from this plasmid and cloned downstream of the constitutive promoter of plasmid pSB13, yielding plasmid pSB13luci. Subsequently, the constitutive promoter was replaced by the L-arabinose inducible promoter *araC*/P_{BAD} (P_{BAD}) (Guzman et al., 1995). For this purpose, plasmid pSB13luci was digested with enzymes *Cla*I/*Sma*I, and ligated to the P_{BAD}-harboring fragment obtained by *Cla*I/*Nae*I cleavage from plasmid pHL259 (Loessner et al., 2007), giving rise to plasmid pSB13P_{BAD}luci (Figure S3A). For induction, 20 μL L-arabinose solution (20 mg mL^{-1} L-arabinose in PBS, Carl Roth) were dropped onto two spots of each agar plate. After 2 hour incubation, 20 μL luciferin solution (30 mg mL^{-1} D-luciferin in PBS, Synchem OHG) was dropped onto the L-arabinose-induced spots as well as onto two non-induced spots of each plate. Luciferase-mediated bioluminescence emission was measured using the IVIS-Spectrum system and the Living Image 4.1 software (PerkinElmer).

Finally, we replaced the luciferase gene by a cassette expressing the HtrA inhibitory peptide P1 fused to an N-terminal signal sequence for delivery in the periplasm and C-terminal hemagglutinin (HA)-tag for antibody detection (Figure S2F). The 21 amino acid signal peptide (SP) was taken from *Hp* CagL (Conradi et al., 2012). The 21 amino acid peptide inhibitor sequence P1 (TGTLLLILSDVNDNAPIPEPR) was taken from a reported HtrA cleavage site in E-cadherin (Schmidt et al., 2016). The haemaglutinin (HA) tag sequence (YPYDVPDYA) was chosen due to its short sequence and available antibodies for detection (Conradi et al., 2012). Serial dilutions of L-arabinose were used to investigate the induction of P1 expression in *Hp*.

Construction of E-Cadherin-Expressing AGS Cells

E-cadherin-negative AGS cells were stably transduced with a pLenti6/V5 construct expressing the human wild-type E-cadherin cDNA as described previously (Oliveira et al., 2009). The expression of E-cadherin and other junctional markers (α-catenin, β-catenin and p120-catenin) in these cells has been tested by immunofluorescence microscopy. In addition, we have determined the

transepithelial electrical resistance (TER) values of E-cadherin-expressing AGS cells, reaching about 150 Ω/cm^2, which is similar to the values obtained in polarized MKN28 cells (Boehm et al., 2012).

Quantification of IL-8 Cytokines by ELISA

MKN28 cells were incubated for up to 24 hours with *Hp*, and PBS-incubated control cells served as negative control. The culture supernatants were collected and stored at -80°C until assayed. IL-8 concentrations in the supernatants were determined by standard ELISA according to manufacturer's procedures (Becton Dickinson).

TER Measurement and Transwell Infection Studies

MKN28, NCI-N87 and MDCK cells were cultured on 0.33 cm^2 cell culture inserts with 3 μm pore size (Millipore). The cells were grown to confluent monolayers, and then incubated for another 14 days to allow cell polarization (Boehm et al., 2012). TER was measured with an Electrical Resistance System (ERS) (Millipore). Maximum TER values indicated that the cells reached maximal polarity. After apical infection, the numbers of transmigrated bacteria were quantified in aliquots from the basal chambers and counting colony forming units (CFU) on agar plates (Boehm et al., 2015). All infection assays were done in triplicates.

In vitro Cleavage Assays of Occludin and Claudin-8 by HtrA

For *in vitro* cleavage studies, 100 ng recombinant human occludin (H00004950-P01, Abnova) or claudin-8 (H00009073-P01, Abnova) were incubated with 50 ng purified HtrA in 50 mM HEPES buffer at pH 7.4. All cleavage reactions were carried out at 37°C for 16 hours.

Bacterial Cell Binding Assay

Infection of MKN28 monolayers was carried out at a density of 3.5 x 10^5 cells in 6-well plates as described previously (Kwok et al., 2002). After infection, the cells were washed three times with 1 mL of pre-warmed RPMI medium per well to remove non-adherent bacteria. To determine the total CFU corresponding to cell-bound bacteria, the infected monolayers were incubated with 1 mL of 0.1% saponin in PBS at 37°C for 15 min. The resulting suspensions were diluted and plated on GC agar plates. The CFUs were counted after 5 days of incubation.

Cloning and Purification of Recombinant HtrA Protein

Cloning and purification of HtrA from *Hp* strain 26695 was performed as described earlier (Boehm et al., 2012). In brief, the *htrA* gene was amplified from genomic DNA by PCR. Using flanking restrictions sites *Bam*HI/*Eco*RI, the PCR product was ligated into the pGEX-6P-1 plasmid (GE Healthcare Life Sciences) and transformed in *E. coli* strain BL21codon+. For purification of GST-HtrA, *E. coli* were grown in 500 mL TB medium to an OD_{550nm} of 0.6 and the expression was induced by addition of 0.1 mM isopropylthiogalactosid (IPTG). The bacterial culture was centrifuged at 4,000 x g for 30 min and pellets were lysed in 25 mL PBS buffer by sonification. The resulting lysate was cleared by centrifugation and the supernatant was incubated with glutathione sepharose (GE Healthcare Life Sciences) at 4°C overnight. HtrA was eluted with 180 units Prescission Protease for 16 hours at 4°C (GE Healthcare Life Sciences). Cleavage products were analyzed by SDS-PAGE and casein zymography as described below.

Casein Zymography

Casein zymography is a highly sensitive and well-established standard technique to analyze protease activities in biological samples (Snoek-van Beurden and Von den Hoff, 2005). Total cell lysates including HtrA proteins were loaded onto 10% SDS-PAGE gels containing 0.1% casein (Roth) and separated by electrophoresis under denaturing conditions. After protein separation, the gel was renatured in 2.5% Triton X-100 solution at room temperature for 60 min with gentle agitation, equilibrated in developing buffer (50 mM Tris-HCl, pH 7.4, 200 mM NaCl, 5 mM $CaCl_2$, 0.02% Brij35) at room temperature for 30 min with gentle agitation, and incubated overnight at 37°C in fresh developing buffer. Transparent HtrA bands having caseinolytic activity were visualized by staining with 0.5% Coomassie Blue R250 as described (Boehm et al., 2012, 2015).

Antibodies

The following antibodies were used: monoclonal AIIB2 integrin-β_1 (Developmental Studies Hybridoma Bank), monoclonal α-CagA antibody (Austral Biologicals), monoclonal pan-phosphotyrosine α-PY99 (Santa Cruz, USA), rabbit α-ezrin (Santa Cruz), rabbit α-claudin-8 (Thermo Scientific), rabbit α-occludin (Thermo Scientific), rabbit α-*Helicobacter pylori* (Dako) and two monoclonal antibodies directed against the extracellular domain of E-cadherin, H-108 (Santa Cruz) and CD324 (BD Biosciences). α-HA antibodies were purchased from Sigma-Aldrich. HtrA proteins were detected by rabbit polyclonal α-HtrA antisera raised against HtrA peptides DKIKVTIPGSNKEY (#1578) and KERAFTLTLAE (#20555). Rabbit polyclonal α-UreB, α-CagA, and α-GGT antibodies were described previously (Tegtmeyer et al., 2013). The α-VacA antibody (#123) was kindly provided by Dr. T.L. Cover (Nashville, TN/USA). The 11-mer peptides of the non-phospho EPIYA-C motif (C-SPEPIYATIDD) and its phospho-form (C-SPEPI(pY)ATIDD) were used for immunizations of rabbits to produce phosphospecific and non-phosphospecific α-CagA-EPIYA-C antibodies according to standard protocols (Biogenes AG, Germany) (Kwok et al., 2007). Dot blot analyses were used to approve the functionality of the phospho-CagA antibody. For this purpose, the above described phospho- and non-phospho EPIYA-C peptides (as well as the corresponding

peptides for EPIYA-A and EPIYA-B motifs) were immobilized on PVDF membranes according to standard protocols, using the BioDot SF apparatus (Bio-Rad) (Lind et al., 2014). These control blots were shown to the reviewers.

Transmission Electron Microscopy (TEM) and Immunogold Labeling Studies

For TEM studies, we reinvestigated the resin blocks of gastric antral mucosa biopsies taken from 20 dyspeptic subjects, five of which proved *Hp*-negative, as used in a previous study (Necchi et al., 2007). The study has been approved by the Ethics Committee of Fondazione IRCCS Policlinico San Matteo (Pavia, Italy) as a reinvestigation of archival material along the same line (i.e., diagnosis of *Hp*-dependent gastritis) as for the original written consensus. Samples were fixed in Karnovsky's solution (2.5% glutaraldehyde and 2% paraformaldehyde in cacodylate buffer, pH 7.3) followed by 1% osmium tetroxide, and then embedded in Epon-Araldite mixture (Necchi et al., 2007). Ultrathin (~70 nm) sections were processed in accordance with the immunogold procedure, using α-HtrA antibodies followed by colloidal gold-labelled goat anti-rabbit IgG (British BioCell, Cardiff, UK). Best immunogold stainings by TEM were obtained for the α-HtrA (1578) antibody. Parallel TEM investigations were carried out on polarized MKN28 or MDCK cells infected at the apical side with either wild-type *Hp* or P1 peptide-expressing bacteria in the presence of L-arabinose. After 6 or 24 h infection, cell monolayers were fixed and embedded as above. Ultrathin sections were then processed for immunogold analysis. Specimens were analyzed by a Jeol JEM-1200 EX II transmission electron microscope equipped with an Olympus CCD camera (Mega View III).

Field Emission Scanning Electron Microscopy (FESEM)

Samples were fixed with 5% formaldehyde and 2% glutaraldehyde in HEPES buffer (0.1 M HEPES, 0.01 M $CaCl_2$, 0.01 M $MgCl_2$, 10 mM sucrose, pH 6.9) on ice and kept for overnight in a fridge at 7°C. After washing with HEPES buffer and TE buffer (10 mM EDTA, 2 mM EDTA, pH 6.9) samples were dehydrated in a graded series of acetone (10, 30, 50, 70, 90, 100%) on ice for 10 min for each step. Samples in the 100% acetone step were allowed to reach room temperature before another change in 100% acetone. Samples were then subjected to critical-point drying with liquid CO_2 (CPD 300, Leica). Dried samples were covered with a gold/palladium (80/20) film by sputter coating (SCD 500, Bal-Tec) before examination in a field emission scanning electron microscope Zeiss Merlin using the Everhart Thornley HESE2-detector and the inlens SE-detector in a 25:75 ratio at an acceleration voltage of 5 kV. For gaining access to transmigrated bacteria through the cell layer critical-point dried samples were fractured with the help of a small piece of adhesive tape by pressing the adhesive tape firmly onto the sample and then lift of the tape using an adapted published protocol (Crull et al., 2011). The newly exposed sample surfaces on the tape and cover slip were again sputter coated with gold-palladium before examination.

Immunohistochemistry (IHC)

Fifty FFPE (formalin-fixed, paraffin-embedded tissue) human gastric biopsy specimens were taken from the diagnostic files of the Institute of Pathology of the Friedrich-Alexander-University Erlangen-Nuremberg. These specimen consisted of 20 antral mucosa samples without *Hp* infection (m:f 14:6, mean age 78.5, range 45-91), and nine antral mucosa samples with *Hp* infection (m:f 3:6, mean age 78.3, range 51-92). All samples were derived from gastric carcinoma bearing mucosa late in the carcinogenesis. These specimens had at least weak gastritis signs, of which the nine *Hp*-positive cases had active and chronic gastritis, whereas the other 20 were rather from the *Hp*-negative atrophic gastritis spectrum with intestinal metaplasia. Microscopic analysis was performed on bioptic areas where *Hp* could be co-localized via serial sectioning. The local ethics committee approved the retrospective use of FFPE material (statement 01/18/2012). We used the BenchMark Ultra ICH/IHS Staining Module (Ventana Medical Systems) for IHC staining. Tissue sections were cut, dewaxed and rehydrated. For antigen retrieval, the slides were heat-treated (95°C, 8 min) in ULTRA cell conditioning solution according to manufacturers' recommendations (Ventana Medical Systems). After UV-inhibition, the primary antibody reactions using α-E-Cadherin antibody CD324 (1:2000 dilution) and α-*Helicobacter pylori* antibody (1:200 dilution), respectively, as well as counterstaining with hematoxyline. The intensity of the E-cadherin expression along the mucosa was measured on the IHC photographs given in percentage in 5% incremental steps. Relative E-cadherin ectodomain staining values were checked by the two-tailed Mann-Whitney test.

Immunofluorescence Staining and Confocal Laser Scanning Microscopy (CLSM)

Immunofluorescence staining with different antibodies as shown in each experiment was performed as described (Hoy et al., 2010; Tegtmeyer et al., 2011). Secondary antibodies were labeled with Alexa-488 or Alexa-546 (Invitrogen, Germany), respectively. For nuclei staining, SYTO-59 was used as recommended by the manufacturer's instructions (Thermo Scientific). Samples were analyzed by confocal laser scanning microscopy using a Zeiss LSM 510 Meta confocal microscope. For quantification of the integrin immunfluorescence signal, the respective raw image stacks were deconvolved with Huygens Professional Software (Version 17.04) to generally increase the signal/noise ratio and to improve the resolution. The quantification steps were then performed using Fiji/ImageJ2 of version 2.0.0-rc-43/1.51 (Schindelin et al., 2015). Five representative regions of interest (ROI) were depicted in either the MOCK sample and in *Hp*-infected sample. The respective ROI was then rotated from *xy* to *xz* direction. Thus, three ROIs were then determined. ROI 1 around the IFM signal on the basal side of the cell and ROIs 2 and 3 on the adjacent basolateral IFM signals. Signal intensity was then measured and for ROIs 2 and 3 accumulated. After measuring, five different ROIs in each sample of the respective data were used to calculate the average over these five ROIs. These average intensities then resulted in the intensity ratio between basal and basolateral integrin accumulation detected by immunofluorescence.

SDS-PAGE and Immunoblotting

Bacterial fractions or infected cells were mixed with equal amounts of 2 x SDS-PAGE buffer and boiled for 5 minutes. Proteins were separated by SDS-PAGE on 8% polyacrylamide gels and blotted onto PVDF membranes (Immobilon-P, Millipore). Before addition of the antibodies, membranes were blocked in TBS-T (140 mM NaCl, 25 mM Tris-HCl pH 7.4, 0.1% Tween-20) with 3% BSA or 5% skim milk for 1 hour at room temperature (Zhang et al., 2015). As secondary antibodies, horseradish peroxidase-conjugated α-mouse or α-rabbit polyvalent rabbit and pig immunoglobulin, respectively, were used (Life Technologies). Antibody detection was performed with the ECL Plus chemiluminescence Western Blot kit for immunostaining (GE Healthcare Life Sciences).

QUANTIFICATION AND STATISTICAL ANALYSIS

Quantitation of Signals in Western Blots and Casein Gels

Quantification of band intensities on immunoblots was performed using the Chemicdoc imaging system (BioRad) and indicated the percentage of phosphorylation per sample. As represented in the corresponding figures the strongest band on each gel was set at 100%.

Statistics

All data were evaluated via Student's t test with SigmaPlot statistical software (version 13.0). Statistical significance was defined by $p \leq 0.05$ (*), $p \leq 0.01$ (**) and $p \leq 0.001$ (***).

Cell Host & Microbe, Volume *22*

Supplemental Information

Helicobacter pylori Employs a Unique Basolateral Type IV Secretion Mechanism for CagA Delivery

Nicole Tegtmeyer, Silja Wessler, Vittorio Necchi, Manfred Rohde, Aileen Harrer, Tilman T. Rau, Carmen Isabell Asche, Manja Boehm, Holger Loessner, Ceu Figueiredo, Michael Naumann, Ralf Palmisano, Enrico Solcia, Vittorio Ricci, and Steffen Backert

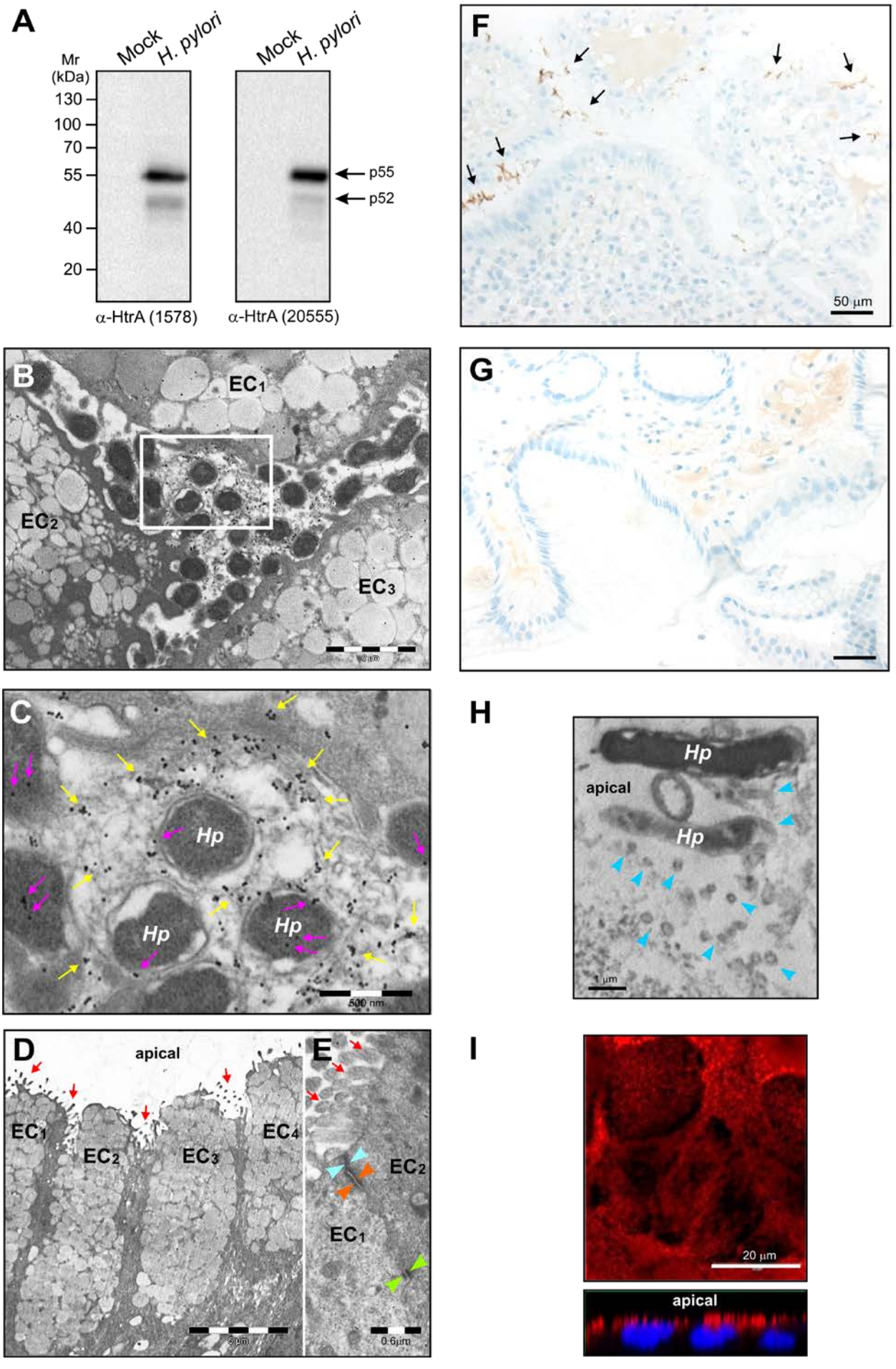
A
Mock
H. pylori
Mock
H. pylori
Mr
(kDa)
130
100
70
55
40
20
p55
p52
α-HtrA (1578)
α-HtrA (20555)
B
EC1
EC2
EC3
C
Hp
Hp
Hp
500 nm
D
apical
EC1
EC2
EC3
EC4
3 µm
E
EC2
EC1
0.6µm
F
50 µm
G
H
Hp
apical
Hp
1 µm
I
20 µm
apical

Figure S1 related to Fig.1. Interaction of *H. pylori* and secreted HtrA with the gastric epithelium *in vivo* and control experiments. (A) Western blots of uninfected MKN28 cells (mock) and MKN28 cells infected with *H. pylori* using two different antibodies directed against HtrA (#1578 and #20555). Both antibodies reacted specifically with the *H. pylori* HtrA bands p55 and p52, but not with other bacterial or host cell proteins. (B) HtrA immunogold labelling of *in vivo* infected gastric epithelial cells. Three epithelial cells are shown (EC_1 to EC_3). A deeply penetrating intercellular cleft is filled with HtrA-positive *H. pylori*. An enlarged section (white box) is shown in (C) and exhibits plenty of HtrA immunogold particles on the bacterial bodies and outer membranes (violet arrows) as well as secreted in the extracellular space (yellow arrows). (D) Transmission electron microscopy of normal non-infected human gastric superficial epithelium *in vivo*. Four mucus-secreting epithelial cells (EC_1 to EC_4) slightly bulging into the lumen are shown. Microvilli structures were detected as indicated (red arrows). (E) High resolution analysis of the *H. pylori*-negative epithelium to demonstrate lack of reactivity for HtrA immunogold particles. Intact luminal microvilli (red arrows) and a well-preserved intercellular junctional apparatus, including tight (blue arrowheads) and adherens (orange arrowheads) junctions as well as a deeply located desmosome (green arrowheads), connecting two adjacent gastric epithelial cells (EC_1 and EC_2) are shown. (F-G) Immunohistochemistry was performed to confirm the *H. pylori* status in all samples. Brown colored bacteria are present in *H. pylori*-positive samples (F), which are absent in *H. pylori*-negative tissues (G). Control experiments for apical cell markers (H-I). Transmission electron microscopy of infected MKN28 cells shows microvilli (blue arrowheads in H) at the apical surface as a bona fide marker of cell polarization. The TEM picture presented here is from the same specimen shown in Figure 4A-B. (I) Polarized NCI-N87 cells were stained with an antibody against the apical marker protein ezrin (red) and nuclear DNA with SYTO-59 (blue).

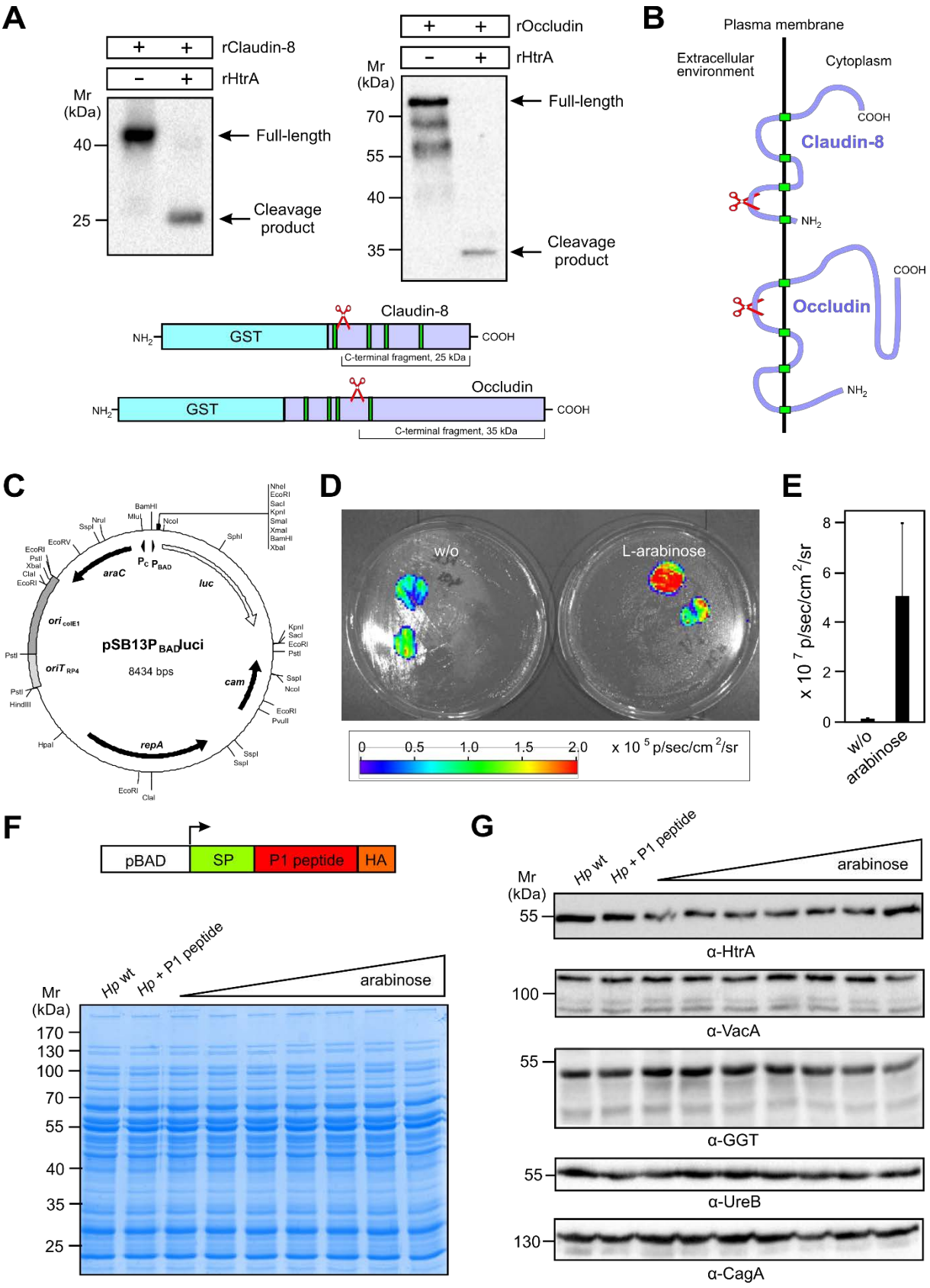

Figure S2 related to Fig.2. *In vitro* cleavage of the purified tight junction proteins claudin-8 and occludin by recombinant HtrA and generation of an arabinose-inducible expression plasmid for luciferase and the HtrA inhibitory peptide P1 in *H. pylori*. (A) *In vitro* cleavage assays of recombinant HtrA (rHtrA) with recombinant GST-tagged claudin-8 (rClaudin-8) or GST-tagged occludin (rOccludin). Full-length and cleaved fragments are indicated with black

arrows. The observed cleavage products correspond in size to the ones observed during infection with *H. pylori* as shown in Figure 2B, suggesting that HtrA can cleave these two proteins at the same positions *in vitro* and *in vivo*. (Bottom) Schematic presentation of recombinant GST-tagged occludin and claudin-8 proteins with indicated sites of transmembrane domains (green) and mapped HtrA cleavage sites (red scissors). (B) Both occludin and claudin-8 contain four transmembrane domains forming two extracellular loops as indicated. The HtrA cleavage sites in these two proteins are located in the first and second extracellular loop, respectively. (C) Plasmid map of the *E. coli/H. pylori* shuttle plasmid pSB13P$_{BAD}$luci. Backbone vector is pSB13, which was constructed based on plasmid pHel2 (Backert et al., 2005). The *ori*$_{ColE1}$ is necessary for replication in *E. coli* and indicated in a region shown in dark grey. The *oriT* sequence of plasmid RP4 (light grey) allows the mobilization of the plasmid from *E. coli* to *H. pylori*. The *repA* gene permits stable replication in *H. pylori* and the *cam* gene cassette allows chloramphenicol resistance for selection. The arabinose-inducible expression system comprises the *araC* gene and pBAD promotor as indicated (Guzman et al., 1995; Loessner et al., 2007). The luciferase (*luc*) gene was placed immediately downstream of pBAD as shown. The arrows indicate the direction of gene transcription. (D) Bioluminescence emission by *H. pylori* strain B8 harboring plasmid pSB13P$_{BAD}$luci was tested on confluent GC agar plates. Twenty µL of L-arabinose (20 mg/mL) were dropped onto two spots of each plate or left untreated on corresponding control plates. After 2 hour incubation, 20 µL luciferin solution (30 mg/mL) were added onto the arabinose-induced spots or two non-induced spots of each control plate. Luciferase-mediated bioluminescence emission was quantified using the IVIS-Spectrum system and the Living Image 4.1 software. (E) Bioluminescence intensities of four spot regions of induced bacteria were compared to four spot regions of non-induced control bacteria. Average radiance was expressed in photons/seconds/cm^2/steradian [p/sec/cm²/sr]. Data are represented as mean ± SEM. (F) Construct showing the E-cadherin-based P1 peptide (Schmidt et al., 2016) fused to an N-terminal signal sequence of gene *cagL* and C-terminal hemagglutinin (HA)-tag for antibody detection. This construct replaced the luciferase gene in pSB13P$_{BAD}$luci and can be induced by the pBAD promotor upon addition of L-arabinose. Expression of peptide P1 can be induced through addition of L-arabinose in a dose-dependent manner by *H. pylori* strain B8, resulting in sustained inhibition of HtrA activity as determined by casein zymography (Figure 3E). As controls, the pattern of total proteins by Coomassie staining (F, bottom) or expression of HtrA and other virulence factors such as GGT, VacA, CagA and UreB remain unchanged as determined by Western blotting (G).

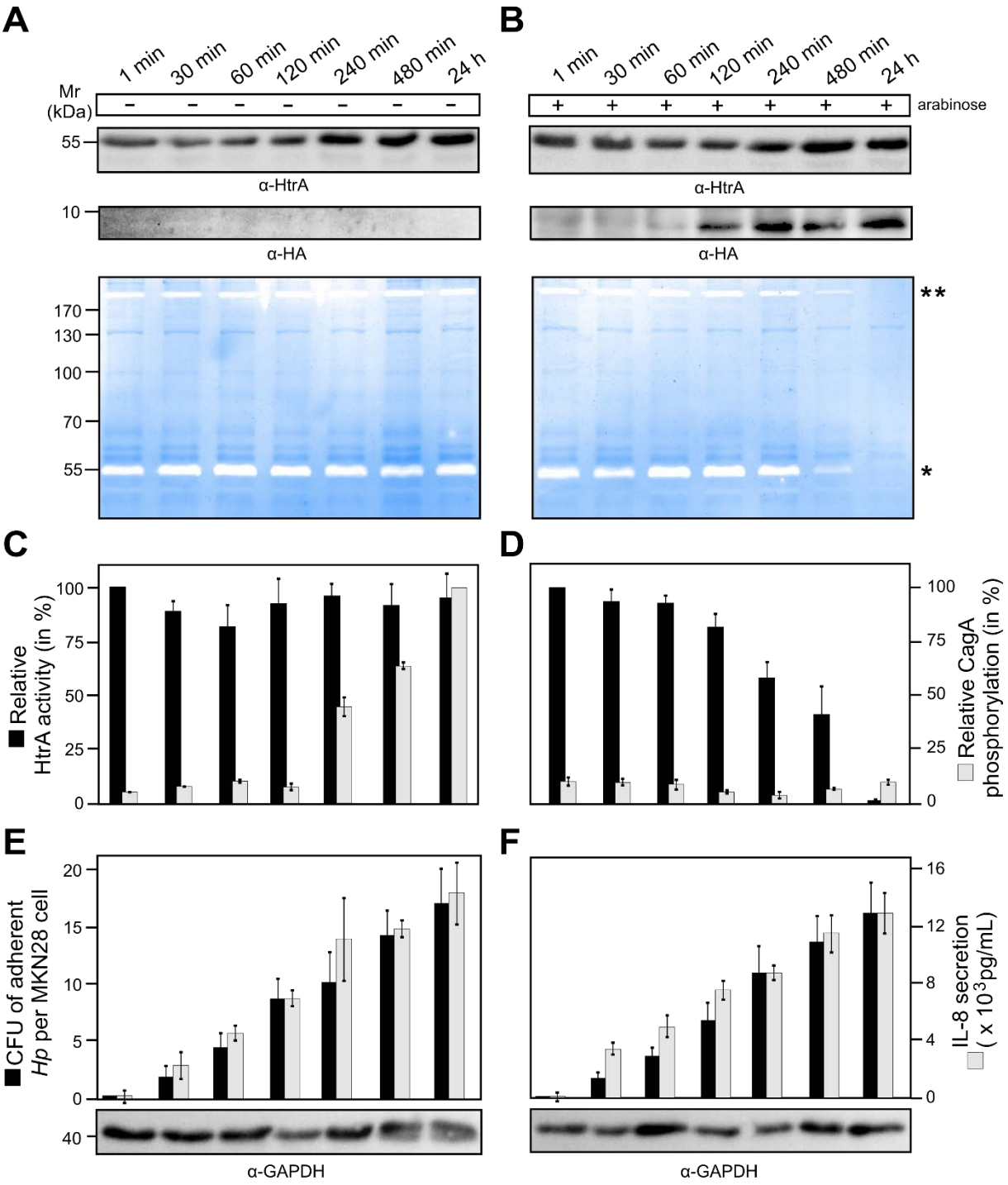

Figure S3 related to Fig. 3. Characterization of *H. pylori* harboring the HtrA inhibitor peptide P1 during infection of polarized MKN28 cells. Differentiated monolayers of MKN28 cells were infected with strain B8 in a time-course up to 24 hours in the absence (A) or presence of L-arabinose (B). The α-HtrA blots show that the amount of HtrA proteins does not change over time and is independent of L-arabinose addition. The α-HA blots indicate that peptide P1 expression is absent in the L-arabinose-negative control (A) and increases over time in the presence of L-arabinose (B). The expression of P1 correlated with the inhibition of HtrA activity over time as judged by casein zymography. Asterisks indicate the position of proteolytically active HtrA monomers (*) and oligomers (**) on the gel. (C) In the absence of arabinose, P1 peptide-encoding *H. pylori* exhibit strong HtrA protease activity and translocate CagA followed by phosphorylation. (D) In the presence of arabinose, P1 peptide-expressing *H. pylori* exhibit decreasing HtrA protease activity, which correlates with abrogation of CagA

translocation and phosphorylation. (E-F) As control, the number of *H. pylori* CFU bound to MKN28 cells and secretion of the cytokine IL-8 was determined over time using the same settings. The results indicate that addition of L-arabinose and inhibition of HtrA did not affect the attachment of the bacteria to the host cells nor T4SS-dependent secretion of IL-8, respectively. Data are represented as mean ± SEM (C-F).

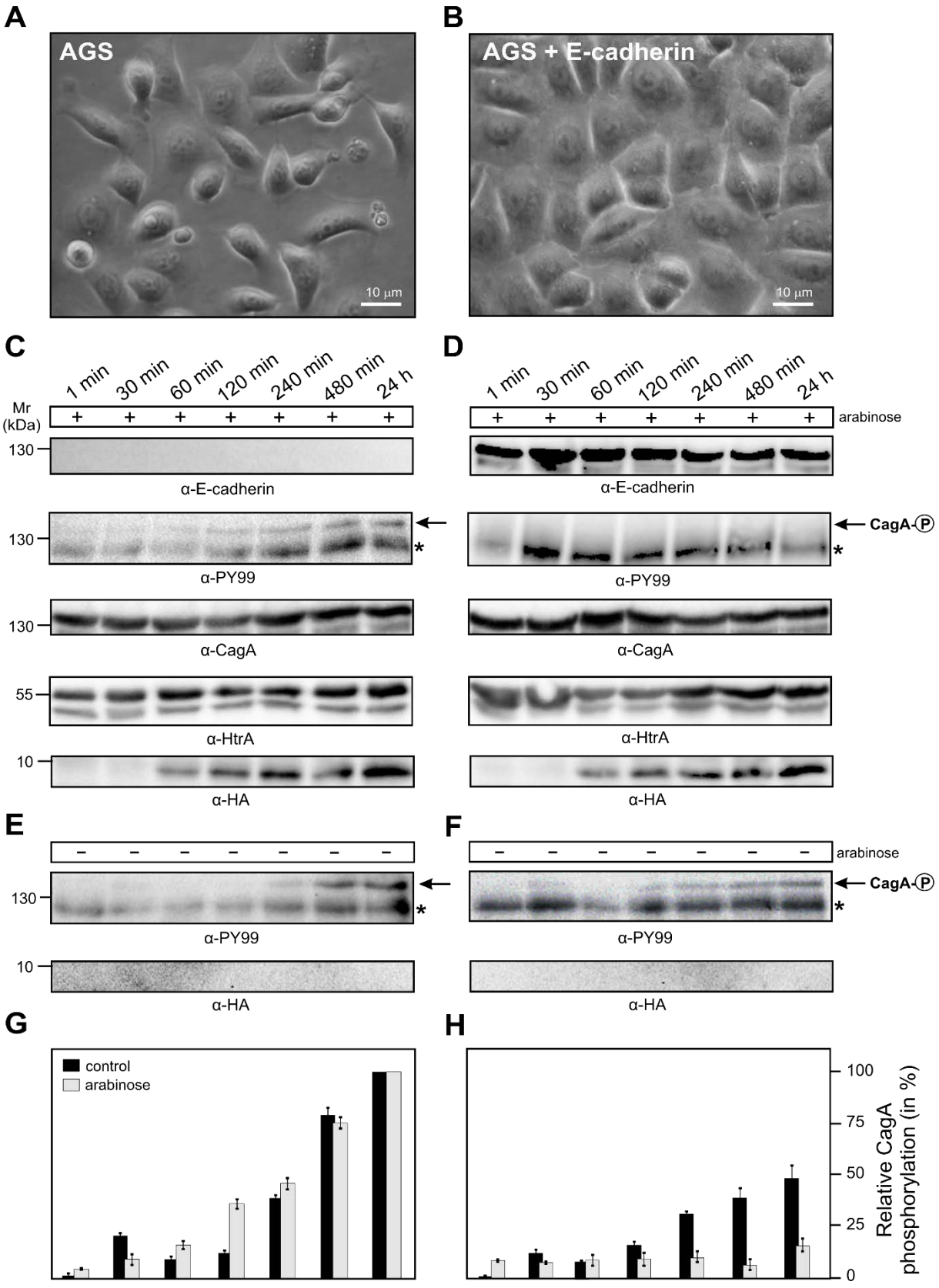

Figure S4 related to Fig.4. Stable expression of E-cadherin in AGS cells changes the cell polarity phenotype and T4SS-dependent CagA translocation by *H. pylori*. (A) Conventional non-polarized AGS cells lack E-cadherin and (B) stable transduction of the *E-cadherin* gene results in a polarized phenotype. (C-D) Infection of E-cadherin-deficient AGS cells with P1 peptide-expressing *H. pylori* strain B8 in the presence of L-arabinose led to

efficient CagA translocation and phosphorylation over time. In contrast, CagA phosphorylation is abrogated during infection of polarized E-cadherin-expressing AGS cells under identical settings. The α-CagA and α-HtrA control blots confirm that equal amounts of protein are loaded. The α-HA blots verify that the P1 peptide inhibitor is expressed under identical conditions over time. (E-F) Control experiment for panel C-D, performed in the absence of arabinose. (G-H) Densitometric quantification of CagA phosphorylation signals in each sample. Data are represented as mean ± SEM.